

Synthesis and Photocatalytic Property of Layered Perovskite Tantalates, $\text{RbLnTa}_2\text{O}_7$ ($\text{Ln} = \text{La, Pr, Nd, and Sm}$)

Masato Machida,* Jun-ichi Yabunaka, and Tsuyoshi Kijima

Department of Applied Chemistry, Faculty of Engineering, Miyazaki University,
Gakuen Kibanadai Nishi, Miyazaki 889-2192, Japan

Received September 9, 1999. Revised Manuscript Received November 23, 1999

The first example of an active layered tantalate photocatalyst containing partly filled lanthanide 4f shell is reported. A single phase of layered perovskite tantalates, $\text{RbLnTa}_2\text{O}_7$, could be obtained with $\text{Ln} = \text{La, Pr, Nd, and Sm}$; the ionic radii of these trivalent cations are required to be larger than 0.126 nm for constructing a perovskite slab. Under UV irradiation from a high-pressure Hg lamp, these layered tantalates demonstrated the photocatalytic activity for water splitting into stoichiometric H_2/O_2 mixtures even without loading metal catalysts. The rates of H_2 and O_2 evolutions were found to be strongly dependent on the lanthanoids, increasing in the sequence of $\text{La} \approx \text{Pr} \ll \text{Sm} < \text{Nd}$. The maximum rate of H_2 evolution observed over $\text{RbNdTa}_2\text{O}_7$ reached $47.0 \mu\text{mol/h}$. The absorption spectrum of $\text{RbNdTa}_2\text{O}_7$ consists of the internal 4f transitions in the visible region and a broad band overlapping the band-gap transition in the UV region. The latter band indicates that a possible excitation process including the partly filled 4f shell plays a key role in photocatalytic reactions. Loading 0.5 wt % Ni onto $\text{RbNdTa}_2\text{O}_7$ by simple impregnation significantly improved H_2 evolution ($117.2 \mu\text{mol/h}$).

Introduction

A variety of mixed metal oxides consisting of TiO_6 , NbO_6 , or TaO_6 octahedral units have been extensively studied as a new class of photocatalysts. The representative catalysts with potential activities for overall water splitting, include SrTiO_3 ,¹ $\text{Na}_2\text{Ti}_6\text{O}_{13}$,² BaTi_4O_9 ,³ $\text{K}_2\text{-Ti}_4\text{O}_9$,⁴ $\text{K}_4\text{Nb}_6\text{O}_{17}$,⁵ $\text{K}_2\text{La}_2\text{Ti}_3\text{O}_{10}$,⁶ and $\text{K}_3\text{Ta}_3\text{Si}_2\text{O}_{13}$.⁷ We have especially noted the use of layered materials because of their possibility of modifying chemical composition as well as microstructure by means of ion-exchange, intercalation, or pillaring, which is useful for designing novel photocatalysts based on semiconducting metal oxide sheets. The concept was first exploited by Domen and co-workers,⁵ who have revealed the presence of an interlayer active site in Ni-loaded $\text{K}_4\text{Nb}_6\text{O}_{17}$. They have demonstrated that pillaring of $\text{KC}_2\text{Nb}_3\text{O}_{10}$ can produce porous photocatalysts with a large surface area.⁸ We have also reported that platinized layered

titanate ($\text{K}_2\text{Ti}_4\text{O}_9$ and $\text{Na}_2\text{Ti}_3\text{O}_7$) showed increased photocatalytic activity after SiO_2 pillaring, because of high dispersion of Pt particles inside the porous texture.^{9,10} Attempts to prepare semiconductor-pillared layered titanate were examined by Sato et al.¹¹ They pointed out that intercalation of semiconductor particles is effective in promoting photocatalytic hydrogen evolution because the recombination between photoinduced electrons and holes was depressed by the electron transfer to a layered host. In such materials, one may consider the interlayer species to form a heterocontact with the oxide sheet, adopting a key role in accelerating photocatalysis of interest. In material viewpoints, therefore, the development of novel ion-exchangeable layered oxides composed of semiconductor sheets is strongly requested in designing highly active photocatalysts.

The present work has been directed toward the synthesis of novel layered perovskite tantalates, $\text{RbLnTa}_2\text{O}_7$ ($\text{Ln} = \text{lanthanoids}$), and evaluation of their photocatalytic activity for overall water splitting. We report here that the evolution of stoichiometric H_2/O_2 mixtures is strongly susceptible to Ln as a result of the participation of Ln4f electrons in the excitation responsible for photoreactions. For the most active catalyst, $\text{RbNdTa}_2\text{O}_7$, the photocatalytic as well as optical absorption properties were discussed from electronic band structure of relevant compounds. The structural modi-

* Department of Applied Chemistry, Faculty of Engineering, Miyazaki University, 1-1 Gakuen Kibanadai Nishi, Miyazaki 889-2192, Japan. Fax: +81-985-58-7312. Telephone: +81-985-58-7323. E-mail: machida@material.chem.miyazaki-u.ac.jp.

(1) Domen, K.; Naito, S.; Ohnishi, T.; Tamaru, K. *Chem. Phys. Lett.* **1982**, *92*, 433.

(2) Inoue, Y.; Kubokawa, T.; Sato, K. *J. Chem. Soc., Chem. Commun.* **1990**, 1298.

(3) Inoue, Y.; Niiyama, T.; Asai, Y.; Sato, Y. *J. Chem. Soc., Chem. Commun.* **1992**, 579.

(4) Uchida, S.; Yamamoto, Y.; Fujishiro, Y.; Watanabe, A.; Ito, O.; Sato, T. *J. Chem. Soc., Dalton Trans.* **1997**, *93*, 3229.

(5) Kudo, A.; Tanaka, A.; Domen, K.; Maruya, K.; Aika, K.; Ohnishi, T. *J. Catal.* **1988**, *111*, 67.

(6) Takata, T.; Shinohara, K.; Tanaka, A.; Hara, M.; Kondo, J. N.; Domen, K. *J. Photochem. Photobiol.* **1997**, *106*, 45.

(7) Kudo, A.; Kato, H. *Chem. Lett.* **1997**, 867.

(8) Domen, K.; *Shokubai* **1992**, *34*, 502.

(9) Machida, M.; Yabunaka, J.; Taniguchi, H.; Kijima, T. In *Preparation of Catalysts VII*; Delmon, B., et al., Eds.; Elsevier: Amsterdam, 1998; p 951.

(10) Machida, M.; Ma, X. W.; Taniguchi, H.; Yabunaka, J.; Kijima, T. *J. Mol. Catal. A: Chem.*, in press.

(11) Fujishiro, Y.; Uchida, S.; Sato, T. *Int. J. Inorg. Mater.* **1999**, *1*, 67.

fications of the layered tantalates by means of ion exchange and metal loading were examined to improve the photocatalytic activity.

Experimental Section

Sample Preparation and Characterization. The $\text{RbLnTa}_2\text{O}_7$ samples with various lanthanoid elements were synthesized by a conventional solid-state procedure according to that reported by Toda et al.¹² for $\text{RbLaTa}_2\text{O}_7$. Powder mixtures of carbonate and oxides (Rb_2CO_3 , Ln_2O_3 (Ln = La, Nd, Sm, Eu, or Tb), Pr_6O_{11} , CeO_2 , and Ta_2O_5 , 99.99%, Rare Metallic Co. Ltd., Japan) were calcined at 1100 °C for 10 h in air. A 50% excess amount of Rb_2CO_3 was used to compensate for the loss caused by volatilization during calcination. As-prepared Rb-type compound was ion-exchanged in molten NaNO_3 at 400 °C to convert into a Na-type and was subsequently washed with distilled water to remove residual nitrate components. Since the resultant tantalate was hydrated in the interlayer, heat treatment at 500 °C was conducted in a stream of dry air to obtain an anhydrous phase. A protonated phase, H-type, was obtained by leaching the hydrous Na-type in 1 mol/L HCl at room temperature for 1 week. The acid solution was refreshed every 2 days. The resultant solid was washed with distilled water and dried at 60 °C in air. The metal-loaded catalyst was prepared by impregnation of as-prepared powders with an aqueous solution of H_2PtCl_6 or $\text{Ni}(\text{NO}_3)_2$ (Wako Pure Chemicals Ind., Ltd., Japan). The impregnated sample was calcined in air at 500 °C. In the case of Ni-loaded catalysts, the sample was then submitted to reduction in a stream of H_2 at 500 °C and subsequent reoxidation in a stream of O_2 at 200 °C. The loading amount of metal was from 0.1 to 2.0 wt %.

The crystal structure of samples was identified by use of a powder X-ray diffractometer (XRD, Shimadzu XD-D1) with monochromated Cu K α radiation (30 kV, 20mA). Diffuse reflectance spectra were recorded with a Jasco V-550 UV-vis spectrometer. The optical band-gap energy was calculated from onset of absorption edges.

Photocatalytic Reaction. The photocatalytic H_2 evolution from water was conducted in an inner irradiation quartz cell, which was connected to a closed gas-circulating system (dead volume: 250 cm³) consisting of a circulation pump, a pressure sensor, gas sampling valves, and stainless steel tubing. A powder sample of the tantalate (0.2 g) was suspended in distilled water (200 cm³) in the cell by use of a magnetic stirrer. Prior to the reaction, the mixture was deaerated by evacuation and then flushed with Ar gas (20 kPa) repeatedly to remove O_2 and CO_2 dissolved in water. The reaction was carried out by irradiating the mixture with light from a 400 W high-pressure Hg lamp. Gas evolution was observed only under photoirradiation, being analyzed by an on-line gas chromatograph (Hitachi, TCD, Ar carrier, MS-5A and Porapak-Q columns). Any contamination from air was confirmed negligible during at least 50 h of photoreactions.

Results and Discussion

Crystal Structure. Figure 1 shows the powder X-ray diffraction patterns of $\text{Rb}_2\text{CO}_3\text{-Ln}_2\text{O}_3\text{-}2\text{Ta}_2\text{O}_5$ systems after calcination at 1100 °C in air. The La compound consisted of a single phase of layered perovskite, $\text{RbLaTa}_2\text{O}_7$, the X-ray diffraction pattern of which were indexed based on tetragonal lattice ($P4/mmm$, $a = 0.3885$ nm, $c = 1.112$ nm) as reported previously.¹² Figure 2 represents the schematic crystal structure of $\text{RbLaTa}_2\text{O}_7$, which is constructed by alternative stacking of a double corner-shared TaO_6 octahedra (perovskite slab) and a monatomic Rb layer along the c axis. Each Rb ion is coordinated by eight oxygens of TaO_6 octahe-

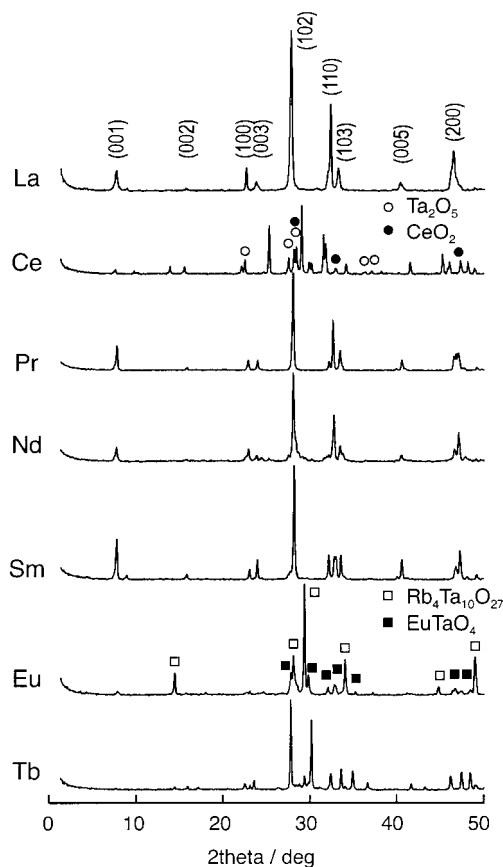


Figure 1. Powder X-ray diffraction patterns of $\text{RbLnTa}_2\text{O}_7$ (Ln = La, Ce, Pr, Nd, Sm, Eu, Tb). The indices are for the layered perovskite phase.

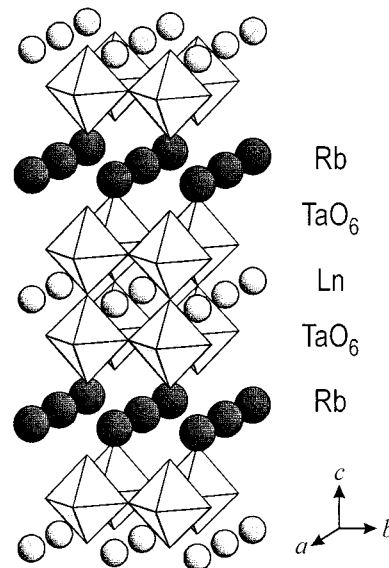


Figure 2. Crystal structure of $\text{RbLnTa}_2\text{O}_7$ with layered perovskite structure.

dra in adjacent two perovskite slabs. This type of tetragonal layered perovskite was also produced for Ln = Pr, Nd, and Sm, being free from the starting materials or other impurities (Figure 1). As can be judged from the shape of diffraction lines, these four samples showed similar crystallinity. Their BET surface areas calculated from N_2 isotherms at -196 °C were in the range of 7–9 m²/g. Table 1 summarizes the crystalline phase in the $\text{Rb}_2\text{CO}_3\text{-Ln}_2\text{O}_3\text{-}2\text{Ta}_2\text{O}_5$ systems and

(12) Toda, K.; Uematsu, K.; Sato, M. *J. Ceram. Soc. Jpn.* **1997**, *105*, 482.

Table 1. Crystal Phase of $\text{Rb}_2\text{CO}_3\text{-Ln}_2\text{O}_3\text{-2Ta}_2\text{O}_5$ System after Calcination at 1100 °C in Air

Ln	r_{Ln}^a (nm)	t^b	crystal phase ^c
La^{3+}	0.1320	0.920	$\text{RbLaTa}_2\text{O}_7$ ($a = 0.3885$ nm, $c = 1.1119$ nm)
Ce^{3+}	0.1290	0.910	CeO_2 , Ta_2O_5 unknown
Pr^{3+}	0.1286	0.909	$\text{RbPrTa}_2\text{O}_7$ ($a = 0.3884$ nm, $c = 1.1115$ nm)
Nd^{3+}	0.1276	0.905	$\text{RbNdTa}_2\text{O}_7$ ($a = 0.3846$ nm, $c = 1.1097$ nm)
Sm^{3+}	0.1260	0.900	$\text{RbSmTa}_2\text{O}_7$ ($a = 0.3842$ nm, $c = 1.1111$ nm)
Eu^{3+}	0.1252	0.897	Eu_2O_3 , Ta_2O_5 , EuTaO_4 unknown
Tb^{3+}	0.1236	0.892	Tb_4O_7 , Ta_2O_5 , TbTa_3O_9 unknown

^a Ionic radius in a 12-coordination site. ^b Tolerance factor, $t = (r_{\text{Ln}} + r_{\text{O}})/(2)^{1/2}(r_{\text{Ta}} + r_{\text{O}})$. ^c Lattice parameters in parentheses are of the tetragonal layered perovskite phase.

lattice parameters of the layered perovskite tantalates. The lattice dimensions, a and c , tend to decrease with the contraction of lanthanoid cations. In the other systems containing $\text{Ln} = \text{Ce}$, Eu , and the heavier lanthanoids, the products consisted of mixtures of lanthanoid tantalates, such as EuTaO_4 , unreacted oxides, or unknown phases. For $\text{Ln} = \text{Ce}$, the reduction of Ce^{4+} to Ce^{3+} necessary for compensating the charge neutrality in $\text{RbCeTa}_2\text{O}_7$ probably did not take place during calcination in air. The results suggest that the formation of layered perovskite in the $\text{Rb}_2\text{CO}_3\text{-Ln}_2\text{O}_3\text{-2Ta}_2\text{O}_5$ systems is dependent on the ionic radius of Ln^{3+} . It is well-known that the structural stability of perovskite-type oxides (ABO_3) can be easily estimated by calculating the tolerance factor defined as $t = (r_{\text{A}} + r_{\text{O}})/(2)^{1/2}(r_{\text{B}} + r_{\text{O}})$, where r_{A} , r_{B} , and r_{O} are radii of the respective ions; i.e., t would be unity for the ideal cubic structure.¹³ As shown in Table 1, the value of t for the perovskite slab (Ln-Ta-O) in the present system decreases from 0.920 for $\text{Ln} = \text{La}$ with decreasing ionic radius of Ln^{3+} , and no layered perovskite was produced at $t < 0.90$ ($\text{Ln} = \text{Eu}$ and heavier lanthanoids). The result suggests that the geometrical arrangement in the perovskite slab governs the structural stability even in the layered structure.

Absorption Spectra. Figure 3 shows the UV-vis diffuse reflectance spectra of as-prepared $\text{RbLnTa}_2\text{O}_7$ with layered perovskite structure. The La compound showed a clear absorption edge at around 300 nm, and the corresponding band-gap energy was 3.9 eV, which is very close to that of common perovskite tantalates such as KTaO_3 and NaTaO_3 .¹⁴ This can be explained by the reported band structure of the perovskite tantalate, where $\text{O}2\text{p}$ forms the valence band, $\text{Ta}6\text{s}$ and 6p orbitals form a high-lying antibonding band, and 5d states of Ta occupy the wide intermediate gap.¹⁵ As shown schematically in Figure 4a, the band gap is therefore between the top of the $\text{O}2\text{p}(\text{p}\pi)$ band and the bottom of the $\text{Ta}5\text{d}(t_{2g})$ band. A similar clear-cut but redshifted absorption edge was observed for $\text{Ln} = \text{Pr}$,

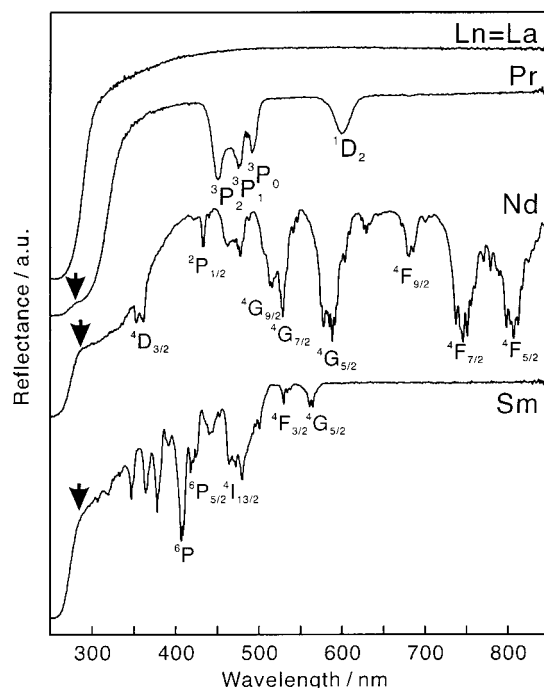


Figure 3. UV-vis diffuse reflectance spectra of $\text{RbLnTa}_2\text{O}_7$. Symbols for each absorption show the excited states of isolated $\text{Ln}4\text{f}$. The ground states are La, 1S_0 , Pr, 3H_4 , Nd, $4\text{I}_{9/2}$, Sm, and $6\text{H}_{5/2}$.

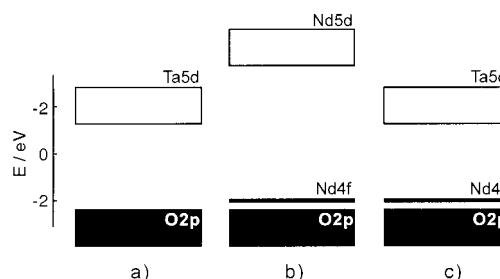


Figure 4. Possible energy schemes for (a) KTaO_3 , (b) Nd_2O_3 , and (c) $\text{RbNdTa}_2\text{O}_7$. Only filled 4f level is shown with neglecting splitting by spin-polarization effect. The band potential is semiquantitative.

where the calculated band gap was 3.5 eV. Although the edge became unclear for $\text{Ln} = \text{Nd}$ and Sm as a result of the overlap with another absorption band, as marked by arrows in Figure 3, their band gaps seem close to that of the La compound (3.8–3.9 eV).

The visible absorption spectra of the tantalate containing from two ($\text{Ln} = \text{Pr}^{3+}$) to five ($\text{Ln} = \text{Sm}^{3+}$) 4f electrons are extremely characteristic. These compounds showed several sharp absorptions with fine structures at >350 nm. As indicated in Figure 3, these absorptions are ascribable to internal transitions in a partly filled 4f shell, so that their positions are basically unchanged regardless of the type of compounds. Actually, the spectra in this region are in accord with those for $\text{Ln}(\text{III})$ hexahalide complexes¹⁶ and simple sesquioxides. This means that the corresponding photoexcitation process is not responsible for photocatalytic reactions described in the following section. These transitions gave rise to narrow absorption bands quite unlike band-gap transitions and are accompanied by vibrational

(13) Goldschmidt, M. *Skr. Nor. Vidensk.-Akad. Kl. 1: Mat.-Naturvidensk. Kl.* **1926**, 8.

(14) Cox, P. A. *Transition Metal Oxides*; Oxford University Press: Oxford, 1992; p 105.

(15) Voorhoeve, R. J. H. *Advanced Materials in Catalysis*; Burton, J. J., Garten, R. L., Eds.; Academic Press: New York, 1977; p 129.

(16) Ryan, J. L.; Jørgensen, C. K., *J. Phys. Chem.* **1966**, 70, 2845.

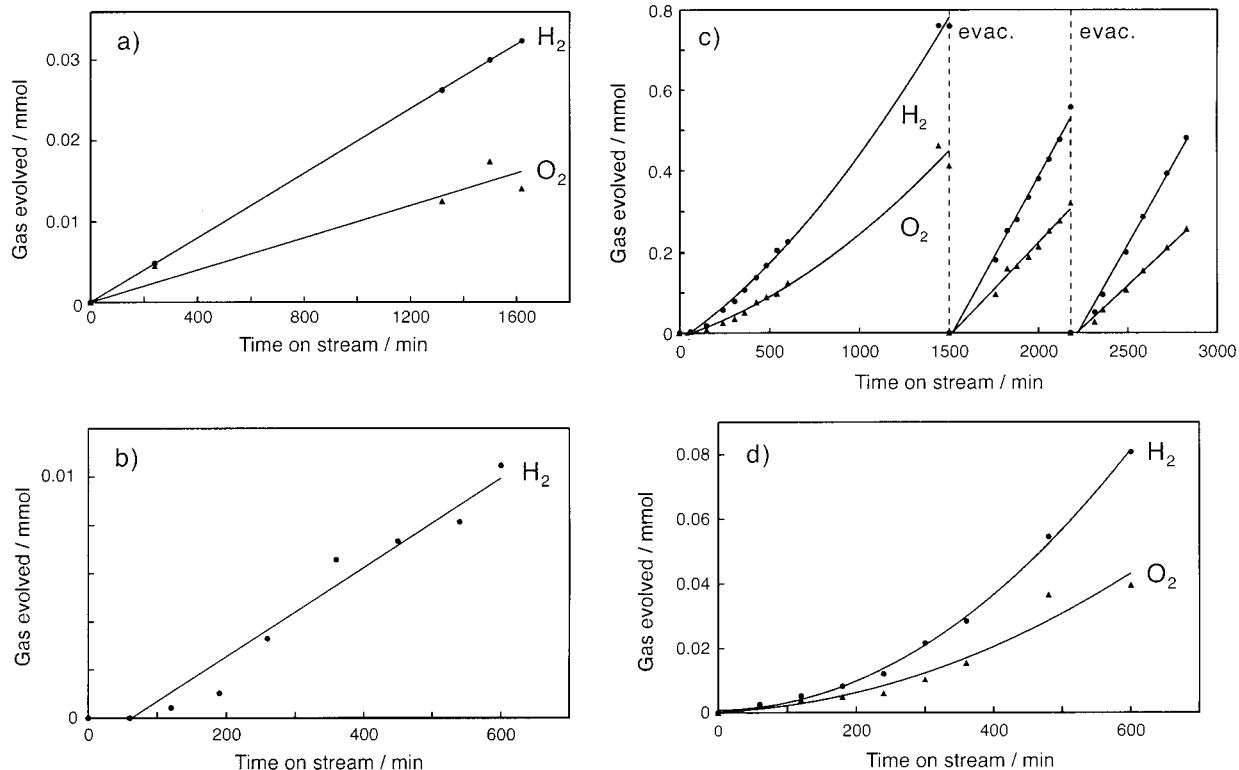


Figure 5. Gas evolution from distilled water over $\text{RbLnTa}_2\text{O}_7$ under irradiation of UV light from a 400W high-pressure Hg lamp. Ln = a) La, (b) Pr, (c) Nd, and (d) Sm. Catalyst 0.2 g, water 200 cm^3 .

structure below and above the wavelength of the electronic lines. Besides the internal 4f transitions, the spectra showed a broad absorption at 300–400 nm overlapping the onset of the absorption edge in the Nd as well as Sm compounds. The redshifted absorption edge observed for the Pr compound (Figure 3) may also come from overlapping of a similar but stronger absorption. These unknown absorptions are not ascribable to the internal transition of Ln4f electrons and the band-gap transition between O2p and Ta5d bands. The origin of this absorption is not clear at this stage, but its relation to the partly filled Ln4f shell is expected from comparison with the spectrum of the La compound having a totally empty 4f shell.

One typical intra-atomic transition concerning 4f electrons is from 4f to 5d. The photoabsorption belonging to the 4f–5d transition, which was reported in hexahalide complexes of Ce and Tb,¹⁶ is not well-established in oxides. Prokofiev and co-workers^{17,18} have studied periodicity in the optical band-gap variation of Ln sesquioxides. According to their recent report,¹⁷ the occupied 4f band in Ce_2O_3 , Pr_2O_3 , and Nd_2O_3 lies above the O2p band (Figure 4b), and thus, 4f–5d transition may determine the band-gap energy. The Ln4f level gradually becomes lowered with an increase of their atomic number, finally lying in the valence band, which results in a monotonic increase of band-gap energy from Ce_2O_3 to Sm_2O_3 . In the present system, however, this is not the case because the conduction band must be mainly composed of Ta5d lying much below Ln5d as shown in Figure 4c. Instead, there are two possibilities

Table 2. Rate of H_2 and O_2 Evolution over $\text{RbLnTa}_2\text{O}_7$

catalyst	rate of evolution ($\mu\text{mol}\cdot\text{h}^{-1}$)	
	H_2	O_2
$\text{RbLaTa}_2\text{O}_7$	1.2	0.6
$\text{RbPrTa}_2\text{O}_7$	0.9	<0.1
$\text{RbNdTa}_2\text{O}_7$	47.0	25.3
$\text{RbSmTa}_2\text{O}_7$	10.6	5.7
Ta_2O_5	0.7	<0.1
Nd_2O_3	0.4	<0.1

of charge transfer transitions involving Ln4f levels, i.e., from the highest filled (valence) band mainly composed of O2p to the Ln4f levels, or from the Ln4f levels to the conduction band. In such cases, the resultant photoexcited electrons or holes may take part in the catalytic reactions on the surface. Actually, however, the direct electron transfers from Ln4f to the conduction band would be impossible due to a large intratomic distance (Ln–Ta: 0.34 nm). In contrast, Ln4f may interact with the O2p (Ln–O: 0.27 nm) that participates in deriving the conduction band through Ta–O–Ta interactions. In this regard, perovskite tantalates can produce the largest overlap between O2p($p\pi$) and Ta5d(t_{2g}).¹⁴ A further discussion must await information about the band structure of $\text{RbLnTa}_2\text{O}_7$, which is now under investigation by means of XPS experiment together with the DV X α molecular orbital calculation.

Photocatalytic Activity for Water Splitting. As-prepared layered perovskite tantalates were applied to photocatalytic decomposition of water without any further pretreatments. Figure 5 shows the time courses of the gas evolution, and data for each rate were collected in Table 2, along with those of several reference catalysts. The $\text{RbLnTa}_2\text{O}_7$ compounds, with the exception of Ln = Pr, produced stoichiometric mixtures of H_2 and O_2 . The amount of gas evolved increased with the

(17) Prokofiev, A. V.; Shelykh, A. I.; Golubkov, A. V.; Smirnov, I. A. *J. Alloys Compd.* **1995**, *219*, 172.

(18) Prokofiev, A. V.; Shelykh, A. I.; Melekh, B. T. *J. Alloys Compd.* **1996**, *242*, 41.

progress of reactions without deactivation. It should be noted that the rate of gas evolution was found to be strongly dependent on Ln^{3+} in the tantalate and decreased in a sequence of $\text{Nd} > \text{Sm} \gg \text{La} \approx \text{Pr}$. In the Nd case (Figure 5c), the rate of H_2 and O_2 evolutions in the first run increased initially with the progress of the reaction, giving rise to 47.0 and 25.3 $\mu\text{mol/h}$, respectively, after 10 h. The first run was terminated by evacuating the reaction system to remove the evolved gas and subsequently introducing 20 kPa of Ar. This was followed by the second and third runs, where the rate of gas evolution at the end of the first run was reproduced. The cumulative amount of H_2 and O_2 evolved during these three runs reached 6.32 and 3.25 mol/mol cat., respectively, suggesting that the reaction proceeded catalytically. We have also carried out the photocatalytic reactions over starting materials, Nd_2O_3 and Ta_2O_5 , as shown in Table 2. Tantalum oxide with a wide band-gap energy of 4.0 eV showed the activity for water splitting, but the rate of H_2 evolved was only 0.7 $\mu\text{mol/h}$. Although no attempts have been examined so far to employ lanthanoid oxides as photocatalysts, 0.4 $\mu\text{mol/h}$ of H_2 evolution was observed over Nd_2O_3 . These reference experiments clearly demonstrate the highly efficient decomposition of water is not due to these possible impurities but is characteristic for the $\text{RbNdTa}_2\text{O}_7$ phase. Although a Degussa P25 catalyst loaded with 0.1 wt % Pt was also applied to the reaction as a reference sample, only H_2 was evolved at the rate $< 0.6 \mu\text{mol/h}$, 2 orders of magnitude less than that of $\text{RbNdTa}_2\text{O}_7$.

The prominent feature of $\text{RbNdTa}_2\text{O}_7$ is the efficient formation of stoichiometric H_2/O_2 mixtures even without loading any metal catalysts such as Pt, Ni, and Cu. This is in complete contrast to conventional photocatalysts, which require an assistance of the metal catalysts to bring about the water splitting. The photocatalyst that can decompose pure water unless loading metal components was reported for $\text{K}_4\text{Nb}_6\text{O}_{17}$,⁵ $\text{K}_3\text{Ta}_3\text{Si}_2\text{O}_{13}$,⁶ $\text{K}_2\text{-La}_2\text{Ti}_3\text{O}_{10}$,⁷ and ZrO_2 .¹⁹ However, the photocatalyst based on layered tantalate perovskite has not been reported so far. Moreover, the present system is the first example of active photocatalysts containing the partly occupied 4f shell. It should be noted that the sequence of activity, $\text{Nd} > \text{Sm} \gg \text{La} \approx \text{Pr}$, is well reflected by the different shape of absorption edge as shown in Figure 3. This is considered largely to be a consequence of the partly occupied Ln4f levels, which form narrow bands within the band gap of the Ta–O sublattice (Figure 4c). This may imply that photoexcited Ln4f electrons play a key role in the photocatalysis of the present layered perovskite tantalates. Clearly, however, further detailed study is necessary to understand the best activity of the Nd compound.

Effect of Modification on Photocatalytic Activity. One promising advantage of the layered tantalates system is a wide variety of possible structural modifications that can be made by means of stepwise exchange of interlayer species. In the first step of this concept, we have evaluated the effect of ion exchange on the photocatalytic activity of $\text{RbNdTa}_2\text{O}_7$. Figure 6 shows the powder X-ray diffraction patterns of Rb-, Na-, and

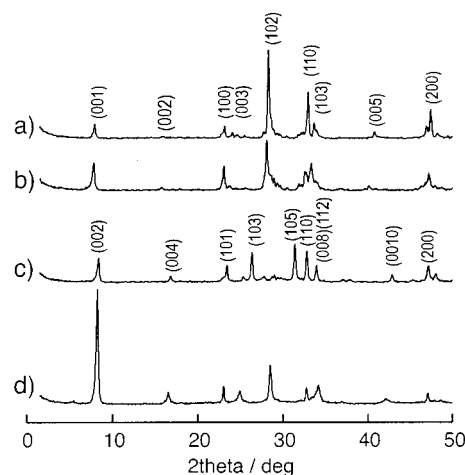


Figure 6. Change of powder X-ray diffraction patterns in stepwise exchange process. a) as prepared $\text{RbNdTa}_2\text{O}_7$, (b) after exchange by Na^+ , (c) b) calcined at 500 °C in dry air, (d) after exchange by H^+ .

Table 3. Effect of Ion Exchange on Photocatalytic Gas Evolutions from Distilled Water

catalyst	rate of evolution ($\mu\text{mol}\cdot\text{h}^{-1}$)	
	H_2	O_2
$\text{RbNdTa}_2\text{O}_7$	47.0	25.3
$\text{NaNdTa}_2\text{O}_7$ (hydrated)	2.4	< 0.1
$\text{NaNdTa}_2\text{O}_7$ (dehydrated)	6.6	4.4
HNdTa_2O_7 (hydrated)	1.4	< 0.1

H-types. The exchange by Na^+ (90%) was accompanied by the shift of the (001) reflection to the lower angles (Figure 6b). The TG/IR analysis showed the resultant larger interlayer distance is brought about by 1.5 mol/mol of water accommodated into the interlayer space. Heating this hydrous phase to 500 °C in the stream of dry air produced anhydrous $\text{NaNdTa}_2\text{O}_7$ (Figure 6c), but the diffraction peaks were indexed with a body-centered lattice ($I4/mmm$). This structural deviations from $P4/mmm$ to $I4/mmm$ was as same as that in the $\text{RbLaTa}_2\text{O}_7$ system reported by Toda et al.,¹² who have revealed that Na exchange causes displacement of a adjacent perovskite slab by $a/2$ along the [110] direction. On the other hand, a 95%-protonated phase (H-type) derived from hydrous $\text{NaNdTa}_2\text{O}_7$ showed the diffraction pattern that can be indexed with the original P lattice (Figure 6d). The ion-exchange processes did not bring about significant changes in BET surface area and microstructure in SEM observation.

Table 3 compares the rate of photocatalytic H_2 evolution of each exchanged phase. The activity of Na^+ - and H^+ -types in hydrous form was very low as compared to that of $\text{RbNdTa}_2\text{O}_7$. However, the Na-type restored the activity after dehydration at 500 °C. These results suggest that ion exchange as well as hydration of the present layered tantalate is not effective in improving the photocatalytic activity. Interestingly, the effect of hydration is in complete contrast to that of the layered photocatalysts, such as $\text{K}_4\text{Nb}_6\text{O}_{17}$ ⁵ or $\text{K}_2\text{La}_2\text{Ti}_3\text{O}_{10}$,⁶ the hydrated forms of which are highly active for overall water splitting. Interlayer space of these compounds is easily hydrated to produce active sites responsible for O_2 evolution. By contrast, $\text{RbNdTa}_2\text{O}_7$ was found to be anhydrous even after dispersion in water. From simple comparison with the reported layered photocatalysts,

therefore, the interlayer space of the present tantalate system is unlikely to take part in gas evolution reactions. Further structural modification by intercalation of oxide precursors into the layered tantalate is now in progress. The resultant pillared layered structure, capable of creating nanocomposites between different metal oxides in porous framework, is expected to be a useful strategy for the development of excellent photocatalysts, which cannot be achieved in other semiconducting oxides with three-dimensional structure.

We have also evaluated the effect of loading metal catalysts to improve the photocatalytic activity of $\text{RbNdTa}_2\text{O}_7$. Although we began with loading 0.1 wt % Pt, it destroyed the activity (rate of H_2 evolved: $1.2 \mu\text{mol/h}$). The XRD measurement suggested that Pt in this case was dispersed on the outer surface of the tantalate. According to the report by Domen et al.,²⁰ the photocatalytic activity of $\text{K}_4\text{Nb}_6\text{O}_{17}$ for water cleavage was improved by incorporating Pt catalysts inside the interlayer but depressed when Pt particles were located at the external surface due to the reverse reaction from evolved H_2 and O_2 to produce H_2O . A partially oxidized nickel catalyst (NiO_x), which has been reported as an active component for water splitting,²¹ was next employed for loading. Figure 7 represents the rate of H_2 and O_2 evolved over the catalyst with various Ni loading. The activity increased with increasing the loading up to 0.5 wt % Ni, at which the rates of H_2 and O_2 evolved reached 117.2 and $58.7 \mu\text{mol/h}$, respectively. A further increase of Ni loading decreased the activity because considerable photoabsorption by NiO_x inhibits the photoexcitation of the tantalate. The role of NiO_x in the photocatalytic decomposition of water was proposed by Domen et al.²² According to their report on $\text{NiO}_x/\text{SrTiO}_3$ photocatalyst, there are two possible photoexcitation routes: one is the band-gap transition in SrTiO_3 and subsequent electron transfer to NiO_x surface, and the other is the band-gap transition in NiO_x .

(20) Sayama, K.; Tanaka, A.; Domen, K.; Maruya, K.; Ohnishi, T. *J. Phys. Chem.* **1991**, *95*, 1345.

(21) Domen, K.; Naito, S.; Soma, M.; Ohnishi, T.; Tamaru, K. *J. Chem. Soc., Chem. Commun.* **1980**, 543.

(22) Domen, K.; Kudo, A.; Ohnishi, T. *J. Catal.* **1986**, *102*, 92.

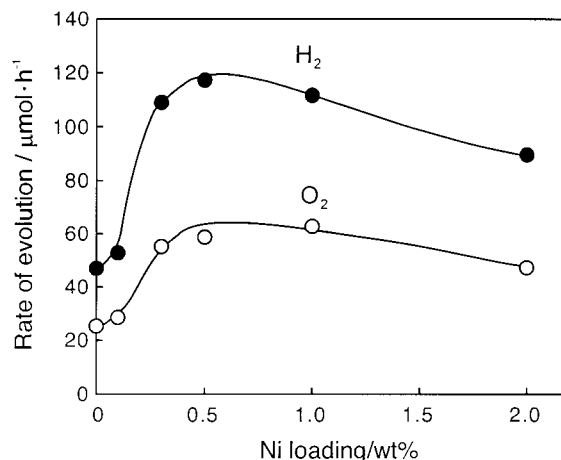


Figure 7. Effect of Ni loading on the photocatalytic evolution of H_2 and O_2 over $\text{RbNdTa}_2\text{O}_7$ under irradiation of UV light from a 400 W high-pressure Hg lamp. Catalyst 0.2 g, water 200 cm^3 .

In both cases, NiO or Ni metal deposited on a NiO surface act as a catalyst for reduction of H^+ to evolve H_2 .

Consequently, this study has revealed the first photocatalysts based on layered tantalate, $\text{RbNdTa}_2\text{O}_7$, for overall splitting of pure water. One striking feature of the $\text{RbNdTa}_2\text{O}_7$ catalyst is that the rapid production of stoichiometric H_2/O_2 mixtures does not require an assistance of loaded metal catalysts. This is completely different from the conventional photocatalysts represented by TiO_2 . We have also found a marked contrast observed in the activity as well as absorption spectra in the isomorphous layered perovskite tantalates with different Ln ions. We have pointed out that electronic interactions including partly occupied Ln4f levels may cause a difference in photocatalytic activity.

Acknowledgment. One of the authors gratefully acknowledges the financial support from Tokuyama Science Foundation and Salt Science Research Foundation.

CM990577J